

Design, Fabrication and Implementation of a Novel Multi Parameter Control Microfluidic Platform for Three-Dimensional Cell Culture and Real-Time Imaging

Vernella Vickerman¹, Jennifer Blundo², Seok Chung³, Roger D. Kamm^{3,4}

¹Department of Chemical Engineering, Massachusetts Institute of Technology, Cambridge, MA, USA

²Department of Mechanical Engineering, Stanford University, Stanford, CA, USA

³Department of Biological Engineering, Massachusetts Institute of Technology, Cambridge, MA, USA

⁴Department of Mechanical Engineering, Massachusetts Institute of Technology, Cambridge, MA, USA

Supplementary Material

Optimization of gel cage geometry

The “gel cage” contains an array of micro-pillars which serves two main functions. Firstly, it permits the delivery and precise localization of small volumes of injectable scaffold material. During microinjection the liquid scaffold is confined within this region due to surface tension. Secondly, once the liquid scaffold has polymerized the micro-pillars provide additional mechanical support. The mechanical stability of hydrogels in the 3D- μ FBR is dependent on the geometry of the “gel cage” region. In previous designs which consisted of a “regular array” of micro-pillars, gels would fracture (Supplementary Fig. 1c) as a result of small pressure differentials across the “gel cage”. The optimized geometry that is presented in this paper, lends mechanical stability and the gels used in the present study are able to withstand pressure differences up to ~ 200 Pa.

PDMS surface treatment facilitates scaffold microinjection

Supplemental Figure 2 shows a water droplet on (a) untreated PDMS and (b) PDMS that was treated with air plasma. A reduction in the contact angle (125° to 21°) allows for favorable wetting dynamics which permits scaffold spreading and filling during microinjection of gel solution. Supplementary Fig. 2 c-f shows typical scaffold loading results for PDMS surfaces that have been rendered hydrophilic. Optimal microinjection results were obtained for contact angles between 20° - 40° (values obtained from hydrophobic recovery data for water droplet on flat PDMS surface which corresponds to approximately 0.5 to 2 hours following surface modification).

Finite element analysis for diffusion of a non-reactive solute in microfluidic device

Supplementary Figure 3 shows simulation results for the distribution of a non-reactive solute (in our gradient experiments, 40kDa dextran) in the “gel cage” region. Dirichlet boundary conditions were prescribed at the inlets for both sink ($C_{\text{sink}} = 0$) and source ($C_{\text{source}} = 1$) channels, continuity at the scaffold interface and zero-flux condition at all other surfaces. A diffusion coefficient ratio ($D_{\text{gel}}/D_{\text{fluid}}$) of 0.1 was assumed for finite element simulations. Normalized intensity values along a line (drawn diagonally to avoid micro-pillars) in the gel region were obtained, the resultant normalized intensity from two fixed points on this line (indicated by * and ** in supplementary Figure 3) were recorded for different simulation times. The results obtained (two different gel cage geometries) were compared to experimental results (obtained in a similar manner) in Figure 2d of the main text.

Simultaneous control for fluid flow and gradients

To demonstrate the multi-parameter control capability of our microfluidic platform, gradients studies were performed with convective flow (hence surface shear stress e.g. on a monolayer) in the microfluidic channels. Here the fluid flow (fixed flow rate controlled by a syringe pump) is perpendicular to the diffusion direction across both lateral surfaces of the gel cage, thus constantly replenishing the sink and source channels to a fixed concentration. The setup consists of two reservoirs that are connected at the base by a long tube (3mm ID Tygon tube, Cole Palmer) which facilitates rapid equilibration of reservoir fluid height thus eliminating any pressure differential across the gel region. This ensures that the evolution of the concentration gradient in the gel region is due to diffusion and not convection through the gel. In addition, the equilibration tube is long enough to avoid contamination of the sink reservoir with fluorescent dextran. A similar procedure to the one presented in the main text was used to analyze fluorescent micrographs. Supplemental Figure 4 shows the results from these experiments. Panel a, shows results (from a single device) of the time evolution of the concentration profile up to 6 hours. A steady state profile is reached and maintained for several hours. To visually demonstrate that there is flow in the channel (while establishing a gradient), fluorescent particles were added to the source reservoir (at $t = 15$ hours) and fluorescent images taken at 1 second intervals. Supplemental Figure 4b shows the localized increase in fluorescence intensity associated with the streaks made by the moving particles within the channels. The baseline intensity in the channel remains relatively constant as well as the sustained gradient (intensities obtained along the dashed line) in the gel. Application of Interstitial flow through three dimensional scaffolds

Supplementary Figure 5 shows the reservoir set-up for imposing pressure differentials across the three-dimensional gel scaffold. The ability to isolate the two microfluidic

channels is demonstrated in panel (a), which shows the microfluidic device with two different color fluid streams. Three-dimensional collagen gels were formed as described in the main text. To ensure easy visualization of liquid column levels, green and red food coloring dye were added to PBS. The upstream (with higher liquid column) reservoir (2.5cm tall Tygon tube, 4mm ID, connected to reducing connector 1/8"X 1/16" ID, Cole Palmer) was colored red and the downstream colored green. At the beginning of each experiment equal volumes of PBS were added to the upstream and downstream reservoirs, and the system was allowed to equilibrate for approximately 2 hours before imposing the pressure differential. Following equilibration, the pressure differential was set (100 Pa or 50 Pa), and mineral oil (M5904, Sigma) was added to all liquid columns to prevent evaporation (these experiments were done outside of the incubator). Supplemental Figure 5b-e shows images of the liquid reservoirs at different time points during the course of the experiment. The devices were oriented such that the downstream and upstream reservoirs were directly in front of each other. The resulting contrast (due to the difference in colors) made it relatively easy to track the evolution of the liquid column levels. The dashed lines indicate the levels of upstream and downstream liquid levels. Figure 2d in the main text shows the result from three separate experiments; two with an initial pressure differential of 100 Pa and one with 50 Pa.

Time-Lapse Video-Microscopy

Microvascular endothelial cells sprouting movie

Supplementary movie 1 and 1b shows the dynamics during sprouting from an intact endothelial cell monolayer.

Movie 1: Initial invasion starts ~6 hours after stimulation with growth factors. Highlights include filopodial dynamics and nucleus translocation into protruding filopodia. Note that structures are in various degrees of focus due to their 3-dimensional nature.

Movie 1b: This is a continuation of movie 1. Highlights include observation of cell proliferation on monolayer and lumen-like structure formation and progression

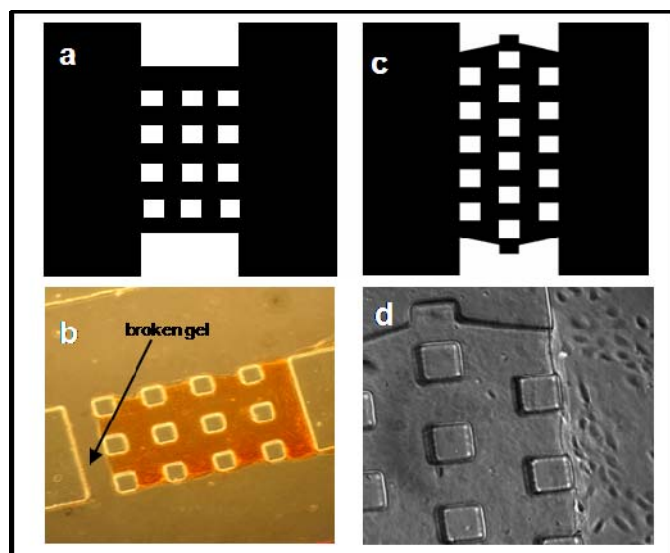
Vacuole dynamics during 2D migration

Movie 2

Perfusion of vascular structures with fluorescent beads

Movie 3: Shows fluorescent beads flowing through a network of endothelial tube structures. A suspension of beads was perfused through the channel in which cells were initially seeded. The endothelial network that developed (after several days in

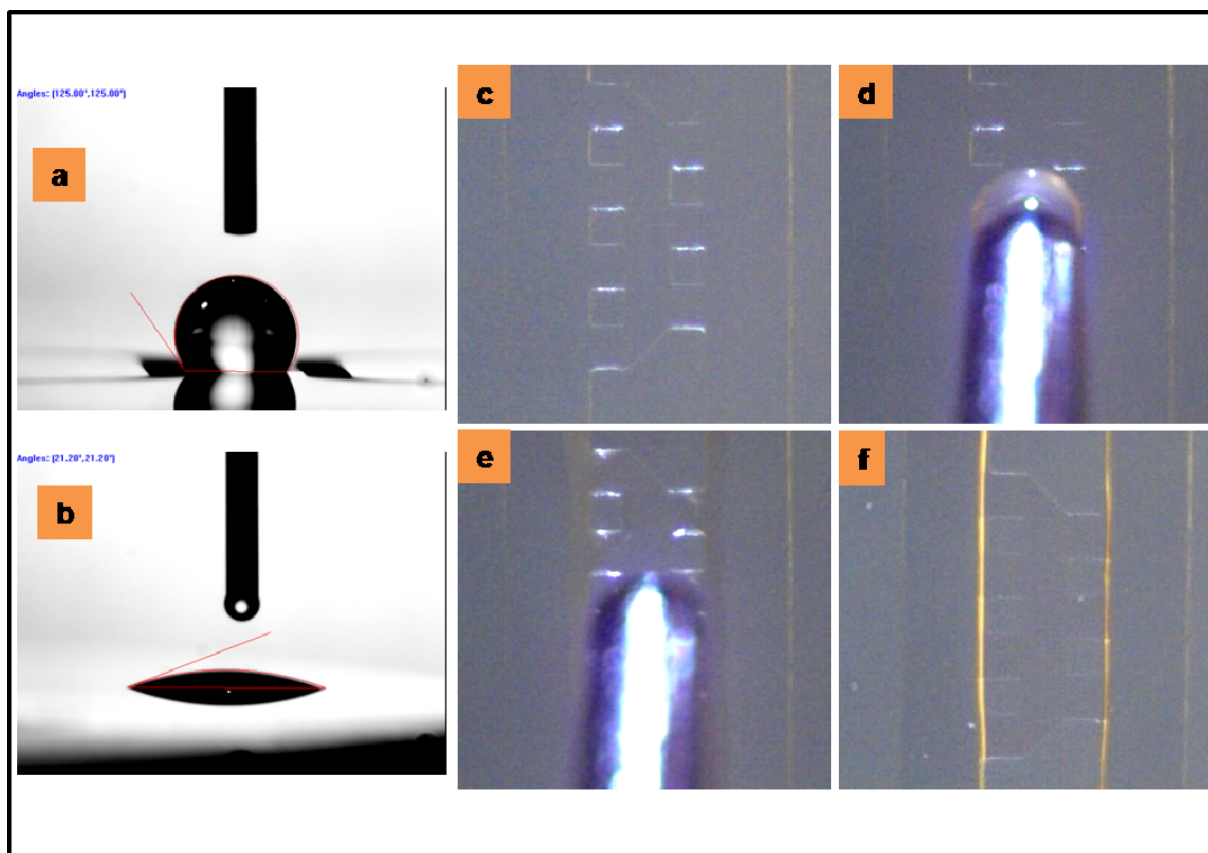
culture) resulted in a direct connection between the two channels thus allowing perfusion of the beads through the vascular network.



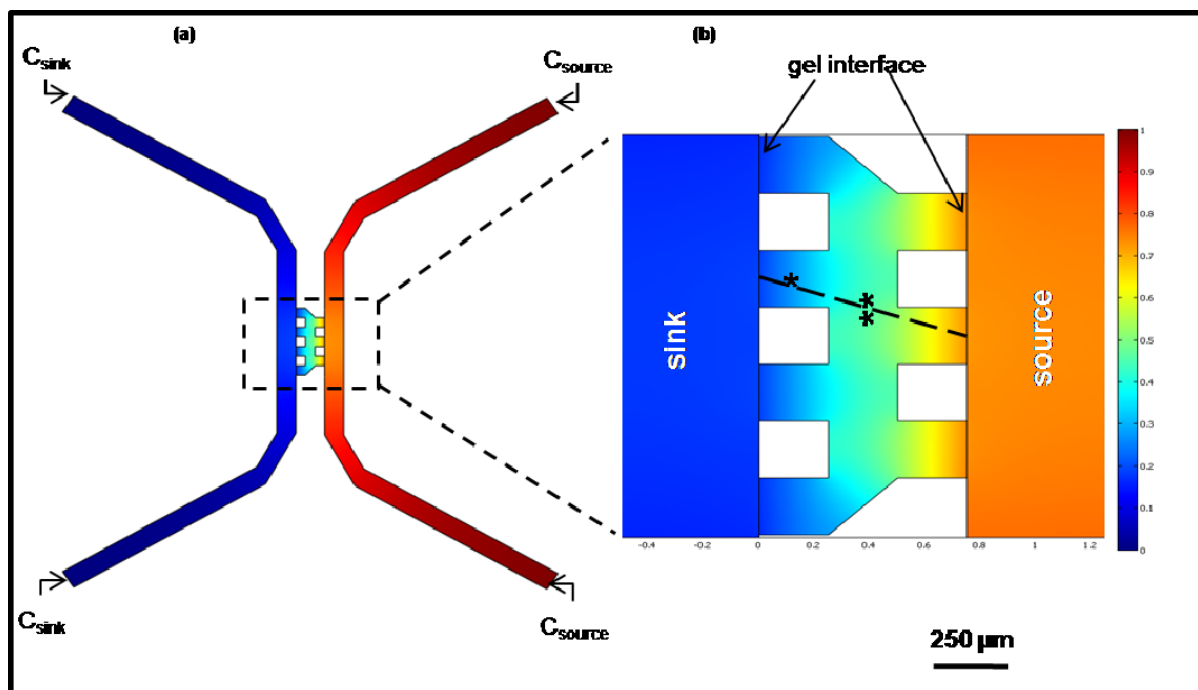
Supplementary Figure 1: Gel cage geometry. Micrographs showing gel cage layouts, “regular array” – (a) and (c) and “staggered array” – (b) and (d) of the 3D- μ FD “gel cage” (micro-pillar 100 μ m x 100 μ m). In panels (c) and (d) the gel cage is filled with a self-assembling hydrogel.

Device label	Micro-pillars (μ m)	Gel cage (μ m)	Channel height (μ m)
A	100 x 100	1000 x 1100	120
B	100 x 100	500 x 1100	120
C	250 x 250	1250 x 1750	240
D*	250 x 250	750 x 1750	240

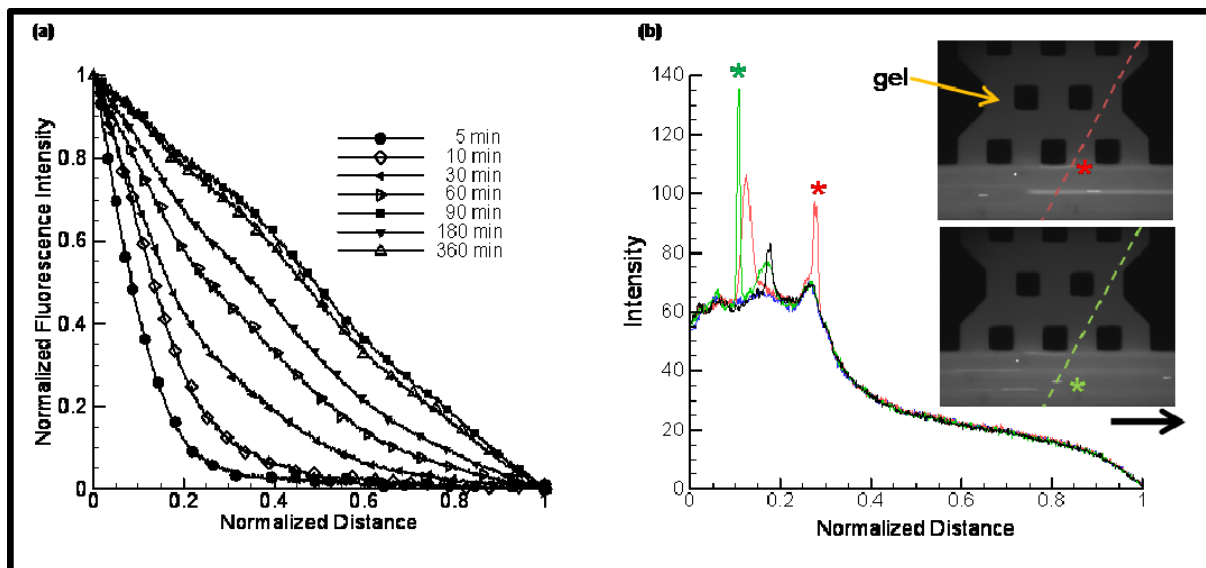
Supplementary Table 1: Dimensions for microfluidic network. Microfluidic channels are 500 μ m wide x 2 cm long. * The gel cage for device D is asymmetric with short side measuring 500 μ m. The number of micro-pillars in gel cage differs for each device: A-28, B-16, C-8 and D-5.



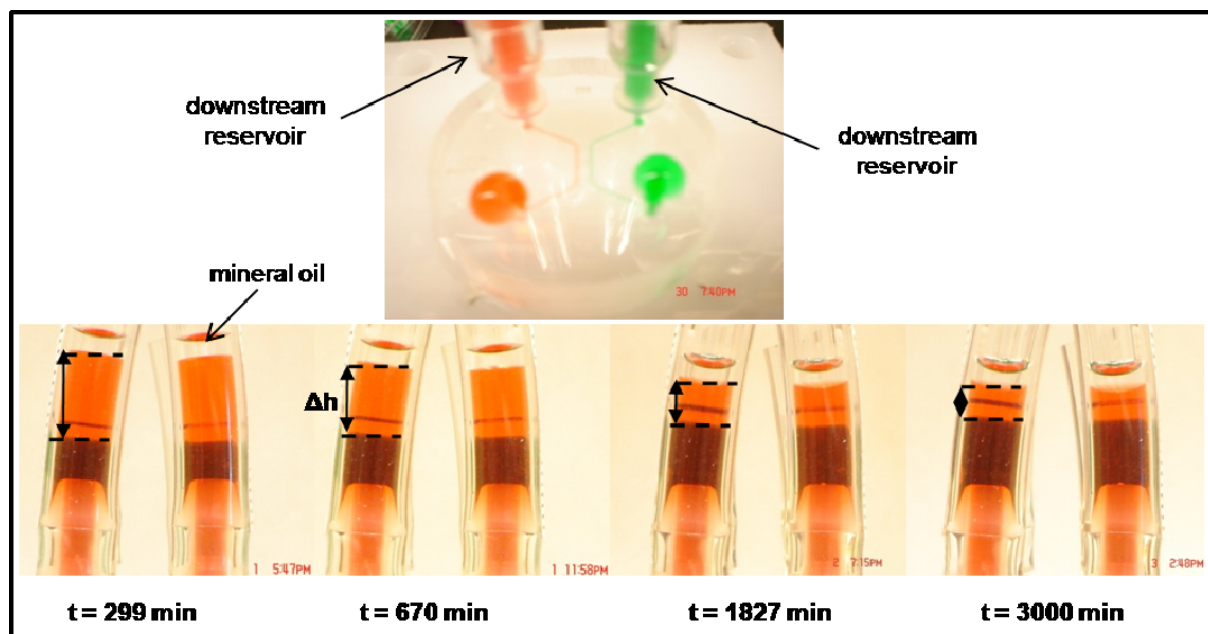
Supplementary Figure 2: Scaffold delivery into microfluidic device via microinjection procedure. Water droplet on (a) native PDMS (hydrophobic) and (b) plasma treated PMDS (hydrophilic). Panels (c)-(f) illustrate microinjection procedure, (f) channels sealed with glass coverslip; sharp line at the liquid-air interface is due to light diffraction (image taken prior to gelation at 37°C).



Supplementary Figure 3: Distribution of a non-reactive solute in scaffold cage. (a) 2D surface map showing results from finite element solution. Concentration of dextran obtained by assuming diffusion coefficient ratio ($D_{\text{gel}}/D_{\text{fluid}} = 0.1$ and $D_{\text{gel}} = 4 \times 10^{-7} \text{ cm}^2 \text{ s}^{-1}$). (b) Concentration distribution in gel region. Dashed line indicates the path (avoiding micro-pillars) from the sink to source channel for which concentrations are used to compare to experimental results. Concentrations at points * and ** along diagonal line were used to generate Figure 2(d) in main text.



Supplementary Figure 4: Evolution on the concentration profile across the “gel cage” with a constant flow rate in microfluidic channels. (a) Normalized average fluorescent intensity. (b) Transients obtained within a few seconds of each other. Spikes in intensity indicate streaks made by particles that flow past the gel region. Dashed line indicates the path along gel and channel for which intensities are recorded. Red and green stars (*) on micrographs (same device at two different time points) indicate the position of beads and corresponding spike in intensity; arrow denotes flow direction.



Supplementary Figure 5: Evolution of liquid pressure differential across “gel cage” induces interstitial flow through the three-dimensional scaffold. (a) Photo of microfluidic device, two microfluidic streams separated by three-dimensional gel scaffold. (b) Photos of liquid level in reservoir at four different time points during the course of the experiment (50 hrs). Dashed line indicates the position of the upstream (red) and downstream (green) reservoir liquid levels. Contrast is due to the orientation the device (reservoirs directly in front each other). Vertical arrows indicate the pressure differential across the scaffold.